

# Temperature dependent effective mass renormalization in 2D electron systems

S. Das Sarma, Victor M. Galitski, and Ying Zhang  
*Condensed Matter Theory Center, Department of Physics,*  
*University of Maryland, College Park, MD 20742-4111*  
 (Dated: May 22, 2019)

We calculate, as a function of temperature and density, the electron-electron interaction induced quasiparticle effective mass renormalization in 2D electron systems within the leading-order dynamically screened Coulomb interaction expansion. We find an unexpected nonmonotonicity in the temperature dependent effective mass with the renormalized mass linearly increasing with temperature at low temperatures and densities. We suggest that this peculiar temperature dependence is a Fermi surface anomaly arising from the ‘soft’ ungapped nature of plasmons in 2D systems.

PACS numbers: 71.10.-w; 71.10.Ca; 73.20.Mf; 73.40.-c

A key insight of the Landau Fermi Liquid theory is that interactions in a Fermi system lead to the renormalization of the single particle fermion mass giving rise to ‘quasiparticles’ with renormalized effective mass whose low energy behavior is qualitatively similar to the corresponding noninteracting free particles [1, 2]. Then, various single particles properties, e.g. specific heat, density of states, etc., in the interacting Fermi system are simply given, at least in the leading-order theory, by replacing the bare (i.e. ‘free particle’) mass  $m$  by the corresponding renormalized effective mass  $m^*$ . In this Letter we present the very *first* microscopic calculation of the *temperature dependent* effective mass renormalization in an interacting 2D electron system (2DES), finding in the process an unexpected nonmonotonic behavior of the effective mass  $m^*(T)$  as a function of temperature in the 2DES. In particular,  $m^*(T)$  first increases almost linearly with temperature in a 2DES reaching a density dependent maximum around  $T/T_F \lesssim 0.5$ , where  $T_F$  is the noninteracting Fermi temperature, after which it decreases with increasing temperature. This nonmonotonic behavior, in particular the temperature induced enhancement of the 2DES quasiparticle effective mass at low temperatures, is entirely unexpected because the naive expectation is that quantum many-body electron-electron interaction effects (underlying the effective mass renormalization phenomenon) should decrease with increasing temperature since the high temperature system is necessarily a classical system. Indeed, the corresponding 3D calculation [2] shows a monotonically decreasing temperature-dependent  $m^*(T)$  at all densities establishing the enhancement of  $m^*(T)$  at low temperature to be a manifestly 2D many-body phenomenon.

Our work is partially motivated by the great deal of recent activity in semiconductor-based 2DES, e.g. Si inversion layers, GaAs heterostructures and quantum wells, etc. where the 2D carrier density can be varied (by tuning an external gate voltage), modifying the strength of the electron-electron interaction usually measured [1, 2] by the dimensionless parameter  $r_s = me^2/(\hbar^2\sqrt{\pi n})$  with  $n$  being the 2D carrier density and  $m$  the bare (i.e. band) mass. The  $r_s$ -parameter [1] in 3D metals (defined with respect to 3D densities) is typically 3 – 5 whereas in

semiconductor 2DES  $r_s$  could vary from 1 (or less) to 20 (or higher), depending on the specific semiconductor system and carrier density being studied. Since the effective mass renormalization scales with  $r_s$  (small and large  $r_s$  respectively corresponding to weakly and strongly interacting electron systems), one expects interesting and important many-body quasiparticle renormalization in 2DES, particularly at large  $r_s$ . It is therefore not surprising that the issue of the effective mass renormalization in 2DES has been extensively studied, both experimentally [3] and theoretically [4, 5, 6, 7, 8] over the last thirty years. All these theoretical studies of quasiparticle mass renormalization have, however, been restricted to  $T = 0$  both in the 2D [4, 5, 6, 7, 8] and 3D [9] system. While this zero-temperature restriction makes perfect sense in 3D systems where the relevant Fermi temperature  $T_F = E_F/k_B$  (defining the temperature scale for the electron system) is extremely high ( $T_F \sim 10^4 K$  in metals), it makes little sense for extremely low density 2DES of current interest [10, 11, 12] where  $T_F \lesssim 1 K$ , making  $T/T_F \sim 1$  in the experimental temperature range. The temperature (and density) dependent effective mass renormalization calculation presented in this Letter therefore takes on additional significance because a number of recent experiments have reported large 2D effective mass renormalization [10, 11, 12] at low densities and low temperatures. We note in this context that the 2D effective mass renormalization  $m^*/m$  in our finite temperature many-body theory is a function of two dimensionless parameter  $r_s$  ( $\propto n^{-1/2}$ ) and  $T/T_F$  ( $\propto n^{-1}$ , since  $k_B T_F = \pi \hbar^2 n/m$  in 2DES), which are however *not* completely independent of each other (since they both depend on the electron density)—in particular,  $T/T_F \sim r_s^2$  for a fixed temperature and changing density.

We consider a 2DES interacting via the long range Coulomb interaction. The effective mass renormalization is microscopically calculated [2] from the electron self-energy function  $\Sigma(\mathbf{k}, i\nu_l)$  defined at the Matsubara imaginary frequency  $i\nu_l$  and 2D wavevector  $\mathbf{k}$ . To calculate the electron self-energy, we make the well-known ‘GW’ approximation [4, 9, 13] of a leading order expansion in the dynamically screened Coulomb interaction (the corresponding Feynman diagram for the self-energy

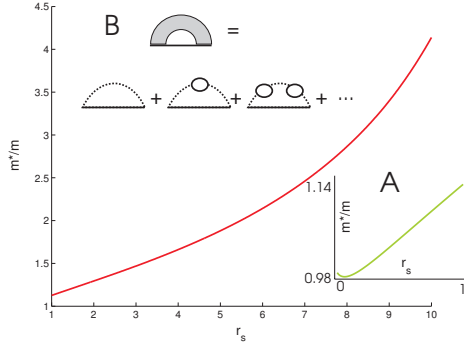


FIG. 1: Calculated  $T=0$  effective mass as a function of  $r_s$  in a 2DES. Inset A provides the result in low  $r_s$  region. Inset B shows the Feynman diagram for the self-energy where the circles are polarization bubbles, the dashed lines the Coulomb interaction, and the solid lines the electron Green's function.

is shown as an inset in Fig. 1), obtaining ( $\hbar = 1$  throughout):

$$\Sigma(\mathbf{k}, i\nu_l) = - \int \frac{d^2q}{(2\pi)^2} T \sum_{\omega_n} \frac{V_q}{\epsilon(\mathbf{q}, i\omega_n)} \cdot \frac{1}{i\nu_l + i\omega_n - \xi_{\mathbf{q}-\mathbf{k}}}, \quad (1)$$

where  $V_q = 2\pi e^2/q$  is the 2D bare Coulomb potential,  $i\nu_l = i(2l+1)\pi k_B T$  and  $i\omega_n = i2n\pi k_B T$  are the usual fermion/boson odd/even Matsubara frequencies ( $l, n$  integers),  $\xi_{\mathbf{k}} = k^2/(2m) - \mu$ ,  $\mu$  the chemical potential, and  $\epsilon(\mathbf{k}, i\omega_n)$  is the RPA dynamical dielectric function, given by the sum of the polarization bubble diagrams:

$$\epsilon(\mathbf{k}, i\omega_n) = 1 - V_q \Pi(\mathbf{k}, i\omega_n), \quad (2)$$

with  $\Pi(\mathbf{k}, i\omega_n)$  the electronic 2D polarizability. Within RPA, we have

$$\Pi(\mathbf{k}, i\omega_n) = 2 \int \frac{d^2q}{(2\pi)^2} \frac{n_F(\xi_{\mathbf{q}}) - n_F(\xi_{\mathbf{q}-\mathbf{k}})}{\xi_{\mathbf{q}} - \xi_{\mathbf{q}-\mathbf{k}} + i\omega_n}, \quad (3)$$

where  $n_F(x) = 1/(e^{x/T} + 1)$  is the Fermi distribution function.

The quasiparticle energy  $E_{\mathbf{k}}$  is obtained from the Dyson equation using the analytically continued retarded self-energy  $\Sigma(\mathbf{k}, i\nu_l \rightarrow \omega + i0^+) \equiv \Sigma(\mathbf{k}, \omega)$ :

$$E_{\mathbf{k}} = \xi_{\mathbf{k}} + \text{Re}\Sigma(\mathbf{k}, E_{\mathbf{k}}). \quad (4)$$

Because we are calculating self-energy to the leading order of dynamically screened interaction, we solve Dyson's equation to the leading order interaction so that perturbation orders are not mixed in the theory:

$$E_{\mathbf{k}} = \xi_{\mathbf{k}} + \text{Re}\Sigma(\mathbf{k}, \xi_{\mathbf{k}}). \quad (5)$$

This approach has previously been used in 2D [4] and 3D [9] zero-temperature effective mass calculations, and

is regarded to be better than solving the full Dyson equation (Eq. 4 above) since it approximately incorporates some vertex corrections. The effective mass can then be derived from the relation  $1/m^* = (k^{-1}dE_{\mathbf{k}}/dk)|_{k=k_F}$ , remembering that the bare band mass  $m$  is given by  $1/m = (k^{-1}d\xi_{\mathbf{k}}/dk)|_{k=k_F}$ :

$$\frac{m^*}{m} = \left[ 1 + \frac{m}{k} \frac{d}{dk} \text{Re}\Sigma(k, \xi_k) \right]^{-1} \Big|_{k=k_F} \quad (6)$$

where  $k_F$  is the Fermi momentum for the non-interacting 2DES.

We use three different techniques in calculating the self-energy: frequency sum, frequency integration, and plasmon-pole approximation. The first two techniques are equivalent to each other, and correspond to different ways of doing the analytic continuation of the imaginary frequency self-energy. The frequency sum technique is explained in Ref. [14], and the frequency integration technique, also called spectral representation, in Ref. [2]. In the frequency sum method, the retarded self-energy is given by

$$\begin{aligned} \text{Re}\Sigma(\mathbf{k}, \omega) = & - \int \frac{d^2q}{(2\pi)^2} V_q n_F(\xi_{\mathbf{q}-\mathbf{k}}) \\ & - \int \frac{d^2q}{(2\pi)^2} V_q \text{Re} \left[ \frac{1}{\epsilon(q, \xi_{\mathbf{q}-\mathbf{k}} - \omega)} - 1 \right] \\ & \cdot [n_B(\xi_{\mathbf{q}-\mathbf{k}} - \omega) + n_F(\xi_{\mathbf{q}-\mathbf{k}})] \\ & - \int \frac{d^2q}{(2\pi)^2} T \sum_{\omega_n} V_q \left[ \frac{1}{\epsilon(q, i\omega_n)} - 1 \right] \\ & \cdot \frac{1}{i\omega_n - (\xi_{\mathbf{q}-\mathbf{k}} - \omega)}, \end{aligned} \quad (7)$$

where  $n_B(x) = 1/(e^{x/T} - 1)$  is the Bose distribution function. For the frequency integration method, the retarded self-energy is

$$\begin{aligned} \text{Re}\Sigma(\mathbf{k}, \omega) = & - \int \frac{d^2q}{(2\pi)^2} V_q n_F(\xi_{\mathbf{q}-\mathbf{k}}) \\ & - \int \frac{d^2q}{(2\pi)^2} \int \frac{d\nu}{2\pi} 2V_q \text{Im} \frac{1}{\epsilon(q, \nu)} \\ & \cdot \frac{n_B(\nu) + n_F(\xi_{\mathbf{q}-\mathbf{k}})}{\nu - (\xi_{\mathbf{q}-\mathbf{k}} - \omega)}. \end{aligned} \quad (8)$$

The plasmon-pole approximation (PPA) is a simpler technique [5, 15, 16] for carrying out the frequency sum in the RPA self-energy calculation by using a spectral pole (i.e. a delta function) ansatz for the dynamical dielectric function  $\epsilon(\mathbf{k}, \omega)$ :

$$\text{Im}\epsilon^{-1}(\mathbf{k}, \omega) = C_k [\delta(\omega - \bar{\omega}_k) - \delta(\omega + \bar{\omega}_k)] / 2, \quad (9)$$

where the spectral weight  $C_k$  and the pole  $\bar{\omega}_k$  of the PPA propagator in Eq. (9) are determined by using the Kramers-Krönig relation (i.e. causality) and the  $f$ -sum rule (i.e. current conservation). We mention that  $\bar{\omega}_k$

in Eq. (9) does *not* correspond to the real plasmon dispersion in the 2DES, but simulates the whole excitation spectra of the system behaving as an effective plasmon at low momentum and as the single-particle electron-hole excitation at large momentum, as constrained by the Kramers-Krönig relation and the  $f$ -sum rule. Details on the PPA are available in literature [5, 15], including the finite-temperature generalization [16]. The PPA, which is known [5, 15, 16] to give results close to the full RPA calculation of self-energy, allows a trivial carrying out of the frequency sum in the retarded self-energy function leading to:

$$\begin{aligned} \text{Re}\Sigma(\mathbf{k}, \omega) = & - \int \frac{d^2q}{(2\pi)^2} V_q n_F(\xi_{\mathbf{q}-\mathbf{k}}) \\ & - \int \frac{d^2q}{(2\pi)^2} V_q C_q \left[ \frac{n_B(\bar{\omega}_q) + n_F(\xi_{\mathbf{q}-\mathbf{k}})}{\bar{\omega}_q - (\xi_{\mathbf{q}-\mathbf{k}} - \omega)} \right. \\ & \left. + \frac{n_B(-\bar{\omega}_q) + n_F(\xi_{\mathbf{q}-\mathbf{k}})}{\bar{\omega}_q + (\xi_{\mathbf{q}-\mathbf{k}} - \omega)} \right]. \quad (10) \end{aligned}$$

We calculate the self-energy by carrying out the 2D momentum integration (Eq. 7, 8, 10) as well as the frequency sum (Eq. 7) and the frequency integral (Eq. 8) in order to obtain the quasiparticle effective mass (Eq. 6). We emphasize that our reason for carrying out our calculation of the electron self-energy by three different techniques (RPA frequency sum and integration, and PPA) is to completely ensure the numerical accuracy of the calculated temperature dependent effective mass by comparing the consistency among the three sets of results. This is particularly significant since there is no existing temperature-dependent effective mass calculation in the literature for us to compare with. The fact that our three sets of results are consistent with each other (and we reproduce the existing [4, 5, 6, 7, 8]  $T = 0$  effective mass results from our finite temperature theory) provides compelling support for our conclusions in this Letter. Since our results obtained in the three techniques are in good agreement, we will only show here our effective mass results using RPA frequency sum method for the sake of brevity.

First, we present our extreme low temperature 2D result ( $T/T_F \approx 10^{-4}$ ) in Fig. 1, to be compared with the existing  $T = 0$  2D results [4, 5, 6, 7, 8], for  $m^*(r_s)$  in the  $r_s = 0 - 10$  range, showing that the effective mass renormalization could be almost as large as 5 for dilute  $r_s \sim 10$  2DES. We emphasize that the results presented in Fig. 1 based on the  $T \rightarrow 0$  limit of our finite temperature theory are in *quantitative* agreement with the existing  $T = 0$  2D RPA effective mass calculations [4] which were, however, restricted to the  $r_s (< 5)$  regime.

In Fig. 2 we show our calculated 2D  $m^*(T)$  as a function of  $T/T_F$  for different values of the 2D interaction parameter  $r_s$  ( $= 1 - 10$ ). In the low temperature region the effective mass first rises to some maximum, and then decreases as temperature increases. This nonmonotonic trend is systematic, and the value of  $T/T_F$  where the effective mass peaks increases with increasing  $r_s$ . The ini-

tial increase of  $m^*(T)$  is almost linear in  $T/T_F$  as  $T \rightarrow 0$ , and the slope  $\frac{d(m^*/m)}{d(T/T_F)}$  is almost independent of  $r_s$  for very small  $r_s$  ( $< 1$ ), but increases with  $r_s$  for larger  $r_s$  values. We mention that we get somewhat stronger temperature dependence (i.e. larger  $dm^*/dT$ ) in our PPA calculation (not shown here).

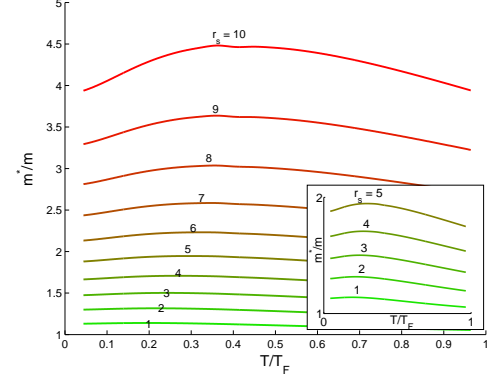


FIG. 2: Calculated 2D effective mass as a function of  $T/T_F$  for different  $r_s$ :  $r_s = 10 - 1$  from top to bottom; Inset:  $r_s = 5 - 1$  from top to bottom. Note that  $T_F \propto r_s^{-2}$ , making the absolute temperature scale lower for higher  $r_s$  values.

In Fig. 3 we show the dependence of the effective mass renormalization as a function of the interaction parameter  $r_s$  for a few values of *fixed* temperature (rather than fixed  $T/T_F$ , remembering that  $T_F \propto r_s^{-2}$  since  $T_F \propto n$  and  $r_s \propto n^{-1/2}$ ). The calculated  $m^*(r_s)$  for fixed  $T$  values is quite striking: For low fixed values of  $T$ ,  $m^*/m$  initially increases with  $r_s$  even faster than the corresponding  $T = 0$  result, eventually decreasing with  $r_s$  at large enough values (where the corresponding  $T/T_F$  values become large enough). This nonmonotonic behavior of  $m^*(r_s)$  as a function of  $r_s$  for fixed temperatures showing a temperature-dependent maximum (with the value of  $r_s$  at which the  $m^*$  peak occurs decreasing with increasing  $T$  as in Fig. 3) is complementary to the nonmonotonicity of  $m^*(T)$  in Fig. 2 as a function of  $T/T_F$  (at fixed  $r_s$ ) and arises from the relationship between the dimensionless variables  $T/T_F$  ( $\propto r_s^{-2}$ ) and  $r_s$  ( $\propto T_F^{-1/2}$ ) due to their dependence on the carrier density (i.e.  $T_F \propto n$  and  $r_s \propto n^{-1/2}$ ).

One immediate consequence of our results shown in Figs. 2 and 3 is that  $m^*(T/T_F, r_s) \equiv m^*(T, n)$  in 2DES could show a strong enhancement at low (but finite) temperatures and low electron densities (large  $r_s$ ). Comparing with the actual system parameters for 2D electrons in Si inversion layers [10, 11] and GaAs heterostructures [12] (and taking into account the quasi-2D form factor effects [8] neglected in our strictly 2D calculation) we find that, consistent with recent experimental findings [10, 11, 12], our theoretical calculations predict (according to Figs. 2 and 3 as modified by subband form factors)  $m^*/m$  to be enhanced by a factor of 2 – 4 for the experimental densities and temperatures used in re-

cent measurements [10, 11, 12]. Due to the approximate nature of our theory we do not further pursue the comparison with experimental data in this Letter leaving that for a future study.

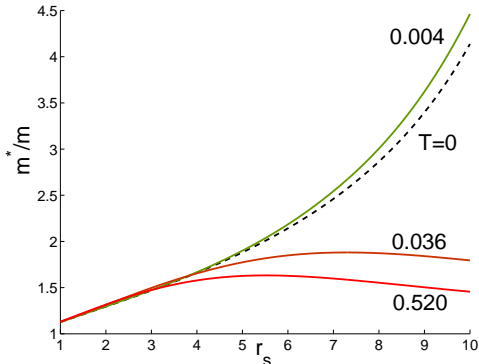


FIG. 3: Calculated  $m^*/m$  at fixed values of temperatures.  $T$  is in the unite of  $T_F$  at  $r_s = 1$ .

The important issue now is identifying the physical mechanism underlying the highly nontrivial nonmonotonicity and the temperature-induced enhancement in 2D  $m^*(T)$ . We believe that the nonmonotonicity in the 2D effective mass renormalization reported in this paper is a Fermi surface anomaly associated with the 2D Coulomb interaction, akin to the corresponding effective mass nonmonotonicity in 3D Fermi liquids associated with electron-phonon interaction in metals [2] and electron-paramagnon interaction in normal He-3 [17]. Such Fermi surface anomalies arise in Fermi liquids if the fermionic interaction in the system is mediated by some soft bosonic mode of the appropriate dispersion and strength. In the 3D example cited above, the soft boson mode mediating the interaction between two fermions is the acoustic phonon for 3D metals [2] and the paramagnon for normal He-3 [17]. In the interacting 2DES of our interest, the relevant soft boson mode is the 2D plasmon mode which, unlike the 3D plasmon mode, is not gapped at long wavelengths ( $q \rightarrow 0$ ), having a long wavelength ‘soft’ dispersion  $\omega_P(q) \sim q^{1/2}$ . (The corresponding 3DES does not exhibit any Fermi surface anomaly arising from Coulomb interaction since the 3D plasmon is not soft, having a gap at  $q = 0$ .)

Motivated by the above considerations we have attempted an analytic calculation of the temperature-dependent 2D effective mass in the leading order dynamically screened interaction. This turns out to be an ex-

tremely difficult task due to the highly complicated non-analytic structure of the integrand in Eq. (1), or equivalently Eqs. (7) or (8). We have only been able to carry out our analytical work in the high-density ( $r_s \ll 1$ ), low temperature ( $T/T_F \ll 1$ ) limit obtaining

$$\frac{m^*}{m} = A(r_s) + B(r_s)T + C(r_s) \left( \frac{T}{T_F} \right)^2 \ln \left( \frac{T}{T_F} \right), \quad (11)$$

where  $B(r_s) \approx B_0 > 0$  for  $r_s \ll 1$ , ensuring that the leading-order temperature correction, in agreement with our numerical results, enhances the effective mass renormalization in a linear manner as  $T \rightarrow 0$ . The sub-leading temperature correction (i.e. the  $T^2 \ln(T/T_F)$  term in Eq. (11)) is also consistent with our numerical results. Note that the  $r_s$ -independence of  $B(r_s)$  found in our analytic theory ( $r_s \ll 1$ ) agrees with our numerical results of Fig. 2. Details on our analytic result and its comparison with our numerical results (and experimental data) will be presented elsewhere.

Finally, we comment on the approximations used in our calculation. First, our theory leaves out quasi-2D form factor (and related solid state physics) effects which are straightforward to include [8] by appropriately modifying the bare interaction  $V_q$  in the theory, and would not lead to any qualitative changes in the results (but would reduce the magnitude of the mass renormalization by a factor of 1.2 to 2 depending on the electron density). Second (and more importantly), our use of the leading-order GW-RPA approximation, which is exact only in the high density ( $r_s \ll 1$ ) limit, is open to question. Although we believe that at finite temperatures the GW-RPA approximation becomes somewhat more accurate (and our quasiparticle energy calculation of Eq. (3) approximately incorporates some vertex corrections going beyond the leading order expansion in the dynamically screened interaction [4, 9]), our principal rationale for carrying out the GW-RPA many-body calculation is that (a) it is the *only systematic* many-body perturbative calculation that is feasible for interacting quantum Coulomb systems; and (b) RPA, while being exact only in the weakly interacting  $r_s \ll 1$  limit, is known to produce qualitatively reasonable results even in the strongly interacting ( $r_s > 1$ ) regime, as demonstrated by the agreement between RPA and experiments in 3D metals ( $r_s \approx 3 - 5$ ) and in 2D semiconductor systems ( $r_s \approx 1 - 10$ ).

This work is supported by NSF-ECS, ONR, DARPA, and LPS.

- 
- [1] D. Pines and P. Nozieres, *The Theory of Quantum Liquids*, (Benjamin, New York, 1966).
  - [2] A. A. Abrikosov, L. P. Gokov, and I. E. Dzyaloshinski, *Methods of Quantum Field Theory in Statistical Physics*, (Prentice-Hall, Englewood Cliffs, 1963).

- [3] J. L. Smith and P. J. Stiles, Phys. Rev. Lett. **29**, 102 (1972); W. Pan, D. C. Tsui, B. L. Draper, Phys. Rev. B **59**, 10208 (1999).
- [4] C. S. Ting, T. K. Lee, and J. J. Quinn, Phys. Rev. Lett. **34**, 870 (1975).

- [5] B. Vinter, Phys. Rev. Lett. **35**, 1044 (1975).
- [6] R. Jalabert and S. Das Sarma, Phys. Rev. B **40**, 9723 (1989).
- [7] H. J. Schulze, P. Schuck, and N. Van Giai, Phys. Rev. B **61**, 8026 (2000).
- [8] T. Ando, A. B. Fowler, and F. Stern, Rev. Mod. Phys. **54**, 437 (1982).
- [9] T. M. Rice, Ann. Phys. (N. Y.) **31**, 100 (1965).
- [10] A. A. Shashkin *et al.*, Phys. Rev. B **66**, 073303 (2002).
- [11] A. A. Shashkin *et al.*, cond-mat/0302004; cond-mat/0301187.
- [12] J. Zhu *et al.*, Phys. Rev. Lett. **90**, 056805 (2003).
- [13] L. Hedin, Phys. Rev. **139**, A796 (1965); J. J. Quinn and R. A. Ferrell, *ibid.* **112** 812 (1958).
- [14] B. Y. K. Hu, Phys. Rev. B **47**, 1687 (1993); B. Y. K. Hu and S. Das Sarma, *ibid.* **48**, 5469 (1993).
- [15] B. I. Lundqvist, Phys. Kondens. Mater. **6**, 206 (1967).
- [16] S. Das Sarma *et al.*, Phys. Rev. B **19**, 6397 (1979).
- [17] D. Balian and D. R. Fredkin, Phys. Rev. Lett. **15**, 480 (1965); D. J. Amit, J. W. Kane, and H. Wagner, *ibid.* **19**, 425 (1967).